(a) Title

NMR study of the influence of pH on phenol sorption in cationic CTAB micellar solutions

(b) List of authors

Paolo Sabatino[a,b], Agnieszka Szczygiel[b], Davy Sinnaeve[b], Maryam Hakimhashemi[a], Hans Saveyn[a], José C. Martins[b] and Paul Van der Meeren*[a]

(c) Affiliations

[a] Particle and Interfacial Technology Group, Faculty of Bioscience Engineering, Ghent University, Coupure Links 653, B-9000 Gent, Belgium.

[b] NMR and Structure Analysis Unit, Department of Organic Chemistry, Faculty of Sciences, Ghent University, Krijgslaan 281 S4, B-9000 Gent, Belgium.

(d) Abstract

Interactions between phenol and cationic cetyltrimethylammonium bromide (CTAB) micelles have been investigated by means of nuclear magnetic resonance spectroscopy. The combined use of ^{1}H and NOESY techniques revealed that phenol has different preferred locations of interaction depending on the pH. At neutral pH (6.70) conditions, phenol molecules are preferentially located in the outer micelle region, at the micelle-water interface, while at more basic pH (9.94), the deprotonated phenol molecules ($C_6H_5O^-$) are immersed into the palisade layer of the micelle. In addition, quantitative estimates of the solubilized fraction of phenol were obtained by using PFG-NMR. The results indicate that the phenol-CTAB interactions, although already present in neutral pH conditions, are largely favored in basic conditions as a consequence of the strong electrostatic interaction between the negatively charged phenolate ions and the positive charge of the cationic surfactant head group.

(e) Keywords

CTAB, phenol, sorption, solubilization loci, ^{1}H-NMR, diffusion spectroscopy, PFG-NMR, NOESY

(f) Corresponding author

Paul Van der Meeren

Tel: +32 (0)9 264 60 03

Fax: +32 (0)9 264 62 42

E-mail: Paul.VanderMeeren@ugent.be

(g) Text

1 Introduction

Solubilization of poorly to moderately water soluble components has been the subject of studies in various fields of application. Thus, this effect forms the basis for the application of concentrated surfactant products in laundry and dish washing. In addition, micellar solubilization has been investigated as a possible formulation strategy for poorly water soluble drugs [1] and it has been proposed as a useful tool in soil remediation [2]. In this application, the micelles should enhance the removal of strongly bound organic compounds during soil washing.

Micellar solubilization may be considered as a partitioning between the aqueous phase and the more hydrophobic interior of the micelle. For various compounds, a close relationship between the micelle-water and the octanol-water partitioning coefficient has been found [3]. For compounds that contain both polar and apolar regions, the interfacial region creates a favorable environment and interfacial, rather than bulk sorption occurs. In addition, additional interactions may further favor solubilization such as the π-cation interaction, as well as electrostatic interactions.

In this manuscript, micellar solubilization of phenol from aqueous solutions was studied in the presence of the cationic surfactant CTAB. The latter was selected since sorption of aromatics is known to be favored by the π-cation interaction [4-7]. Phenol, as well as other small aromatic molecules such as nitrobenzenes, have been found as important contaminants in industrial sites [8-10]. In these cases, micellar solubilization may help to remove phenol and related compounds from the soil by washing. In addition, it may help the further treatment by increasing the retention in membrane processes, which is referred to as micellar enhanced ultrafiltration (MEUF) [11-13]. In this contribution, we focus on pH effects, which will affect the acid-base equilibrium of phenol. Whereas the increased polarity of phenol upon dissociation might hamper micellar solubilization, the increased electrostatic interaction with cationic micelles might be expected to generate a promoting effect. The final balance between both effects was investigated using NMR methodology, focusing both on the sorption site, and the amount of sorption.

2 Materials and Methods

2.1 Materials

The cationic surfactant cetyl trimethylammonium bromide (CTAB, MW=364.45 g/mol, >99% pure) was purchased from Acros Organics. Phenol (MW=94.11 g/mol, 99% pure) was obtained from Sigma. Sodium hydroxide (MW=40 g/mol, 99% pure) was NormaPUR, acquired from VWR Prolabo. Deuterium oxide (D_2O >99.8% atomD) was purchased from Armar Chemicals (Switzerland). 4,4-dimethyl-4-silapentane-1-sulfonate sodium (DSS-d_6, MW=224.32 g/mol, >98% atomD) was acquired from Isotec Inc. All the products were used as purchased and not further purified.

2.2 Sample preparation

Blank samples containing 5 mM phenol in D_2O and 10 mM CTAB in D_2O, as well as a mixture of 5 mM phenol and 10 mM CTAB in D_2O were prepared. A series of samples containing 5 mM phenol with increasing concentrations of sodium hydroxide (0.6, 1.0, 2.0, 4.0, 6.5 mM) as well as a similar series, containing additionally 10 mM CTAB, were prepared in D_2O. After the preparation, the samples were stirred overnight and then used for the NMR measurements during the following two days. The pH of the different samples was measured directly in the NMR tube at 25 °C using a combined pH-meter *Spintrode* electrode purchased from Hamilton.

2.3 Nuclear magnetic resonance spectroscopy

All the NMR experiments were performed on a Bruker Avance II spectrometer operating at a ^1H frequency of 700.13 MHz and equipped with a 5 mm ^1H TXI-Z gradient probe with a maximum gradient strength of 57.7 $G \cdot cm^{-1}$. Measurements were performed at 25 °C and the temperature was controlled to within ±0.01 °C with a Eurotherm 3000 VT digital controller.

For chemical shift measurements, a solution of sodium 4,4-dimethyl-4-silapentane-1-sulfonate (DSS-d_6) in D_2O was used as external reference, from which the chemical shift of the residual HDO was determined to be 4.80 ppm. This value was used as secondary reference throughout all measurements.

NOESY experiments were carried out using a phase sensitive gradient enhanced pulse sequence with z-spoil to eliminate zero quantum coherence [14-16] and 300 ms mixing time.

Diffusion coefficients were measured by PFG-NMR with convection compensated double stimulated echo experiments [17] using monopolar smoothed rectangular shaped gradient pulses and a modified phase cycle to minimise phase distortions due to unwanted gradient echo's [18]. The echo-decay of the resonance intensity obtained with the double stimulated echo sequence obeys equation 1, from which it is clear that the diffusion coefficient D is derived from the echo-decay as a function of the parameter k.

$$I = I_0 \exp\left[-D(\gamma G \delta s)^2 \Delta'\right] \tag{1}$$

$$I = I_0 \exp\left[-D \cdot k\right]$$

where I is the echo intensity with gradient; I_0 is the echo intensity at zero gradient; γ is gyromagnetic ratio; G the maximum gradient amplitude; δ the duration of the gradient pulse and Δ' is the diffusion delay corrected for the finite gradient pulse duration $\Delta' = \Delta - 0.6021 \cdot \delta$. The gradient shape factor s was set to 0.9, to account for the smoothed rectangular gradient shape used here [19]. A detailed description of the PFG-NMR method and the sequences mentioned above, is provided in several excellent reviews [20, 21].

The determination of the diffusion coefficient with corresponding 67% confidence interval was based on the fitting of a mono-exponential curve to the echo decay of the peak intensity of the selected resonances using the Monte Carlo procedure [22]. This fitting procedure was repeated 100 times for each experiment; according to Alper and Gelb [22], 60 fits are sufficient to produce a constant confidence interval.

2.4 Determination of the partitioning into the micelle

When phenol molecules are added to a micellar solution of CTAB surfactant, they are either dissolved in water or solubilised in the micelles. In the former state, phenol diffuses freely in the aqueous phase, whereas upon sorption, the phenol molecules diffuse together with the surfactant aggregates. Assuming the exchange between the micellar and the aqueous phase is fast on the NMR time scale, the chemical shift observed may be expressed as described in equation 2:

$$\delta_{obs} = p \cdot \delta_{sorbed} + (1-p)\delta_{free} \tag{2}$$

where δ_{free} and δ_{sorbed} are the chemical shift values of the molecule of interest in the free and sorbed states, respectively and *p* represents the fraction of the molecules sorbed by the micellar solution.

Similarly, the observed diffusion coefficient D_{obs} of the phenol in the presence of micelles is also averaged according to equation 3 [23]:

$$D_{obs} = p \cdot D_{sorbed} + (1-p)D_{free} \quad (3)$$

where D_{free} and D_{sorbed} represent the diffusion of the free molecules and those sorbed in the micelle. It is then possible to derive the value of the bound fraction p according to:

$$p = \frac{D_{free} - D_{obs}}{D_{free} - D_{sorbed}} \quad (4)$$

3 Results and discussion

3.1 ^{1}H-NMR

The aim of the present study is to investigate the effect of pH on the phenol-CTAB interaction using NMR. Figure 1 shows the ^{1}H-NMR spectra at 25 °C of a 10 mM CTAB solution in D_2O (figure 1a), a 5 mM phenol solution in D_2O with a measured pH of 6.50 (figure 1b) and a mixture of 5 mM phenol and 10 mM CTAB solution in D_2O with a measured pH of 6.70 (figure 1c). In figure 1a, the resonance at 0.93 ppm belongs to the terminal methyl group of the alkyl chain. The intense resonance at 1.35 ppm is representative of the aliphatic methylene groups, while the smaller ones at 1.43, 1.83 and 3.43 ppm belong to the γ, β and α methylene groups, respectively. The single resonance at 3.20 ppm originates from the three methyl groups contributed by the quaternary ammonium group. In figure 1b the doublet at 6.96 ppm represents the ortho-protons, while the two triplets at 7.03 and 7.36 ppm belong to para- and meta-protons, respectively.

When both compounds are mixed (figure 1c) several changes are apparent. First the aromatic region displays two instead of three resonances for the phenol, a simplification resulting from the overlap of the ortho and para resonances. In the CTAB region, a perturbation of the chemical shift to lower values (upfield) for the α-, β- and γ-methylene groups as well as the $-N^+(CH_3)_3$ one was noticed, with the γ-methylene shifting under the resonance of the long aliphatic chain. The latter, together with the terminal methyl group resonance does not appear to be affected by the presence of phenol. This upfield

shift is most likely attributed to ring current shift effects caused by phenol as is well documented in literature [5, 24-27] and may be considered as evidence for the vicinity between both molecules most probably with residence of the phenol at the micelle-water interface, since only the chemical shifts of groups close to the head of the micelle are affected.

To assess the impact of the phenol ionization state on the interaction with CTAB micelles, ^{1}H NMR spectra were recorded varying the pH by addition of sodium hydroxide (section 2.2). Figure 2 shows the ^{1}H-NMR spectra of 5 mM phenol in D_2O at 25 °C in a pH range between 7.22 and 11.40. It is clear that the change in pH perturbs the position of the phenol resonances (figure 4). This effect is particularly marked in the upper traces of figure 2, where the pH of the solutions is comparable (2c) or higher (2d, e) than the pKa of phenol, which is located at 9.89 according to literature [28]. In these conditions the aromatic compound is also present in the phenolate ($C_6H_5O^-$) form.

In figure 3, the effect of pH variation on the chemical shift of phenol (left) and CTAB (right) resonances present in the 5 mM/10 mM mixture is shown. Whereas both the samples with the two lowest and the two highest pH conditions are very similar, figure 3c is intermediate between these two extremes. The measured pH range for this series of samples varied from 8.03 to 12.31, which is slightly higher as compared to the pH range measured in the absence of CTAB. This discrepancy is due to the presence of CTAB which gives rise to a more alkaline environment.

In figure 4 the changes in chemical shift of the aromatic protons, induced by the pH titration, are depicted both in the absence and presence of CTAB. Considering phenol in the absence of CTAB (empty symbols in figure 4), the largest change in chemical shift occurs between pH 9.5 and 10.5, in good agreement with the reported pKa of phenol. In the presence of CTAB, however, this jump, linked to the dissociation of phenol to phenolate, occurs between pH 8.5 and 9.5, i.e. indicating an apparent pKa value [29] of roughly 9 instead of 10. The downward shift in apparent pKa upon sorption in cationic micelles was also observed by Mchedlov-Petrossyan and Kleshcheevnikova [30] and is at least partly due to the fact that the local pH at the micelle-water interface is higher than the bulk pH. In addition, it is known that the dissociation equilibrium may be affected by the molecular environment of the dissociating group.

Table 1 summarizes the pH dependent chemical shift of the CTAB protons. The chemical shift change is expressed as (δ_i-δ_f), where δ_i is the proton chemical shift of CTAB measured in D_2O in the absence of phenol and sodium hydroxide, as shown in figure 1a and δ_f is the chemical shift in the

presence of phenol and NaOH (figure 3). From table 1 it is obvious that the upfield shift of the CTAB moieties augments significantly when the pH approaches the pKa value of phenol in the presence of CTAB, suggesting that the interaction between phenol and surfactant changes to become stronger as the pH increases. When the pH of the solution exceeds the pKa value, even the inner methylene groups and the terminal methyl group appear to be affected, as these experience a less important yet significant downfield change in chemical shift (figure 3d, e). The change of the inner CTAB chemical shifts in a direction opposite to those in the vicinity of the ammonium head of the micelle was explained by Caghi et al. [26], on the basis of the change in electron density of their local environment, once the solubilized molecules penetrate deep into the palisade layer of the micelle. Indeed, the alkyl methylene and terminal methyl groups will experience a more polar environment (as compared to being in contact with other alkyl chains) whereas the quaternary ammonium methyl groups will experience a less polar environment due to a lower hydration upon insertion of (and partial neutralization by) the (partly dissociated) phenol.

Based on this explanation together with the chemical shift evolution already seen, one could propose that when the pH increases, the phenolate ion produced has the ability to deeper penetrate the micelle in such a way that the aromatic ring resides in the upper hydrocarbon region of the micelle while the negative charge carried by the oxygen interacts with the positively charged nitrogen at the head of micelle. For the sake of completeness it is worth mentioning that this behavior is in contrast to the so-called pH-piston hypothesis as described by Avdeef [31] which points to a more outward solubilization locus of solubilized species upon dissociation. This contradiction may be explained by the fact that the phenolate is oppositely charged to the surfactant in this case, which causes the more polar characteristics upon dissociation to be more than compensated by the increased electrostatic interaction, which drives the phenolate inside the micelle. Once the phenol is fully deprotonated, a further increase in pH does not affect the position of the resonances in agreement with this view.

3.2 NOESY

To further probe and confirm the localization of phenol with respect to the micelles as derived from chemical shift arguments, 2D NOESY spectra were measured as a function of pH. Both the negative sign of intramolecular NOE's as well as the presence of intermolecular NOE's connecting resonances of both species can be used to this effect (Figure 5). At pH 6.70, in the absence of any added sodium

hydroxide, no intermolecular NOE peaks are found between aromatic and surfactant protons, and the phenol resonances show weak positive NOE's, that can unambiguously be recognized since typical zero-quantum artifacts between scalarly coupled spins were eliminated using a recently described modification [16]. The lack of intermolecular NOE's signifies that phenol is hardly inserted into the CTAB micelles while the weak positive intramolecular NOE's indicate that the phenol remains in a highly dynamic and solvated form. As proposed before from the chemical shift perturbations, phenol is therefore most probably located at the micelle-water interface. The 2D NOESY spectrum at higher pH (figure 5b) clearly demonstrates that the interaction between phenol and CTAB changes as a function of pH. Indeed, at pH 9.94, the phenol resonances are connected by negative NOE peaks while negative intermolecular NOE's arise between phenol and CTAB resonances. The negative character of these intramolecular NOE cross-peaks indicates a considerable reduction in rotational correlation time for the phenolate molecules, a clear sign of insertion inside the CTAB micelles. The intermolecular NOEs connecting the resonances of phenol and surfactant are clearly visible (figure 5b) except for the terminal methyl group of the long alkyl chain of CTAB. Although a precise positioning cannot be estimated with certainty, the absence of the latter NOE contact indicates that the aromatic ring is probably located in the upper hydrocarbon region of the micelle. In addition, only very weak intermolecular NOE's are observed between the phenolate proton in the para position and the α and β methylene groups of CTAB, which shows that the para group is on average located somewhat further from the micellar surface.

The different solubilization loci of the phenol may be explained on the basis of the different interactions taking place when the pH is varied. At neutral pH the presence of the phenol at the micelle-water interface (figure 6a) is due to the π-cation interaction [4-7]. This observation is in line with the findings of Xu et al. [27] who also found that at neutral pH, phenol accumulates at the micelle-water interface and in the hydrophilic head group region of cetyl pyridinium chloride micelles. At higher pH, the electrostatic interaction between charges of opposite sign may give rise to ion pairing which drives the phenol deeper in the micelle (figure 6b). In this configuration, the ortho and meta protons will be closer by the surface, with para deeper inside the micelles.

3.3 PFG-NMR

The chemical shift and NOE analysis give qualitative information about the different interactions when the pH is varied. With PFG-NMR, quantification of the degree of sorption is possible. According

to equation 4, in fact, to evaluate the sorption of phenol into the micelle, three different diffusion coefficients must be determined. The diffusion coefficients of phenol in the presence (D_{obs}) and absence (D_{free}) of surfactant were determined on the basis of the signal of the aromatic protons, while the diffusion coefficient of the micelles was obtained from the most intense signals, $-N^{+}(CH_3)_3$, $-(CH_2)_{12}$ and ω-CH_3.

The average values of the diffusion coefficients as well as the standard deviations thus calculated are summarized in table 2. It follows from table 2 that the rate of diffusion of phenol in an aqueous solution decreases as function of pH due to the formation of deprotonated molecules. A similar observation was made by Wang et al. [32] for humic acid. The higher diffusion coefficient at lower pH was explained by the more compact geometry upon neutralization of carboxylic and phenolic OH groups. In a CTAB micellar solution, this diffusion rate reduction is even more pronounced as a consequence of the increased amount of molecules sorbed into the micelle. CTAB micelles, on the other hand, diffuse always at the same rate regardless of pH conditions. Using the Stokes-Einstein equation (equation 5) it is possible to deduce the hydrodynamic radius R_H of the CTAB micelles from their diffusion coefficient D_{mic}.

$$R_H = \frac{k_b T}{6\pi\eta D_{mic}} \tag{5}$$

where k_b is the Boltzmann constant, T is the temperature, and η is the viscosity of D_2O (η=1.095 mPa·s at 25 °C). The similar diffusion coefficients found for CTAB, which correspond to a hydrodynamic radius of about 3.2 nm, indicate that no shape changes occur at the phenol concentration used, as described upon benzene solubilisation in CTAB by Hedin et al. [33].

Based on the experimental values of the diffusion coefficients, the percentage of sorbed phenol was calculated from equation 4. It is interesting to note in figure 7 that for values of pH below the pKa of phenol only modest changes in bound fraction were observed, whereas when the pH value is higher than the pKa, the bound fraction rapidly increased to about twice the initial value. In these conditions, a further increment of pH did not have further effects on the degree of sorption. This trend is in line with the observations made about the changes in chemical shift and NOESY experiments and it is a further confirmation that the deprotonated form of phenol has a greater ability to penetrate the micelle. Additionally, the reversibility of the sorption, i.e. the ability of the micelles to release the sorbed phenol when the pH is lowered again, was investigated. Hence, the sample containing 5 mM phenol and 10 mM CTAB at the highest pH condition (pH=12.31) was acidified by addition of formic acid until a pH

value around 3.5 was reached. The diffusion experiment carried out on this new sample showed that phenol diffuses faster and therefore only a small fraction of phenol is still bound to the micelle. The sorbed fraction so calculated was 30±1%, meaning that upon addition of formic acid the bound fraction returns to a value in line with the value found in conditions of neutral pH, meaning that the micelle has the capability to adsorb and release the solubilizate depending on the pH conditions of the solution (figure 7). This opens interesting perspectives for a controlled sorption and desorption, e.g. for micellar enhanced ultrafiltration. In this application, a high degree of sorption is desirable during the filtration phase, whereas a low degree of sorption may enable to recycle the surfactant from the retentate.

4 Conclusions

The present paper illustrates the pH influence on the interaction between phenol and cationic surfactant micelles using different NMR techniques (^{1}H, NOESY and PFG).

On the chemical shift basis, it has been hypothesized that at pH close to neutrality phenol prefers to be solubilized at the micelle-water interface, since only the $N^+(CH_3)_3$, α-CH_2, β-CH_2 and γ-CH_2 groups are affected by the presence of phenol, while at higher pH conditions, the aromatic compound is assumed to be located deeper inside the micelle because also the inner methylene groups of the surfactant tail are influenced.

NOESY experiments strongly supported this hypothesis. At neutral pH, no cross peaks between surfactant and phenol protons appear in the NOESY spectrum, meaning that the spatial correlation between phenol and micelle is rather weak. At higher pH, NOE peaks do exist, originating from a closer spatial correlation between the two molecules, demonstrating that the aromatic compound is located in the palisade layer of the micelle.

Finally, PFG-NMR was used to evaluate quantitatively the fraction of phenol bound to the micellar solution. It was observed that the sorption of phenol increased along with pH, which was explained by the strong electrostatic attraction of the phenolate ions formed. Interestingly, this observed sorption increment was shown to be reversible upon pH cycling.

Acknowledgment

The authors thank the Fund for Scientific Research – Flanders (FWO-Vlaanderen) for a Ph.D. fellowship to Paolo Sabatino and Davy Sinnaeve, as well as for various research and equipment grants (G.0365.03; G.0064.07; G.0678.08; G.0102.08).

References

[1] O.C. Rangel-Yagui, A. Pessoa, L.C. Tavares, Micellar solubilization of drugs, J. Pharm. Pharmaceut. Sci. 8 (2005) 147-163

[2] W. Chu, Remediation of contaminated soils by surfactant-aided soil washing, Pract. Periodical of Haz., Toxic, and Radioactive Waste Mgmt. 7 (2003) 19-24

[3] A. Leo, C. Hansch, D. Elkins, Partition coefficients and their use, Chem. Rev., 71 (1971) 525-616

[4] J. Ulmius, B. Lindman, G. Lindblom, T. Drakenberg, H-1, C-13, Cl-35, and Br-81 NMR of aqueous hexadecyltrimethylammonium salt-solutions – solubilization, viscoelasticity, and counterion specificity, J. Colloid Interface Sci. 65 (1978) 88-97

[5] C.A. Bunton, C.P. Cowell, The binding of phenols and phenoxide ions to cationic micelles, J. Colloid Interface Sci. 122 (1988) 154-162

[6] C. Groth, M. Nyden, K.C. Persson, Interactions between benzyl benzoate and single- and double-chain quaternary ammonium surfactants, Langmuir 23 (2007) 3000-3008

[7] P. Saveyn, E. Cocquyt, D. Sinnaeve, J.C. Martins, D. Topgaard, P. Van der Meeren, NMR study of the sorption behavior of benzyl alcohol derivatives into sonicated and extruded dioctadecyldimethylammonium chloride (DODAC) dispersions: the relevance of membrane fluidity, Langmuir 24 (2008) 3082-3089

[8] C.Z. Katsaounos, E.K. Paleologos, D.L. Giokas, M.I. Karayannis, The 4-aminoantipyrine method revisited: determination of trace phenols by micellar assisted preconcentration, Int. J. Environ. Anal. Chem. 83 (2003) 507-514

[9] W. Frenzel, J. Oleksyfrenzel, J. Moller, Spectrophotometric determination of phenolic-compounds by flow-injection analysis, Anal. Chim. Acta 261 (1992) 253-259

[10] C.L. Kang, Y. Wang, R.B. Li, Y.G. Du, J. Li, B.W. Zhang, L.M. Zhou, Y.Z. Du, A modified spectrophotometric method for the determination of trace amounts of phenol in water, Microchem. J. 64 (2000) 161-171

[11] M. Krivorot, Y. Oren, Y. Talmon, Y. Schmidt, J. Gilron, Characterization of micellar systems for removal by MEUF of refractory organic from contaminated groundwater, Desalination 200 (2006) 718-719

[12] F. Luo, G.-M. Zeng, J.-H. Huang, C. Zhang, Y.-Y. Fang, Y.-H. Qu, X. Li, D. Lin, C.-F. Zhou, Effect of groups difference in surfactant on solubilization of aqueous phenol using MEUF, J. Hazard. Mater. 173 (2010) 455-461

[13] J. Juri, J.S. Yang, S.H. Kim, J.W. Yang, Feasibility of micellar-enhanced ultrafiltration (MEUF) for the heavy metal removal in soil washing effluent, Desalination 222 (2008) 202-211

[14] J. Jeener, B.H. Meier, P. Bachmann, R.R. Ernst, Investigation of exchange processes by 2-dimensional NMR-spectroscopy, J. Chem. Phys. 71 (1979) 4546-4553

[15] R. Wagner, S. Berger, Gradient-selected NOESY – A fourfold reduction of the measurement time for the NOESY experiment, J. Magn. Reson. Ser. A 123 (1996) 119-121

[16] M.J. Thrippleton, J. Keeler, Elimination of zero-quantum interference in two-dimensional NMR spectra, Angew. Chem. Int. Ed. 42 (2003) 3938-3941

[17] A. Jerschow, N. Muller, Suppression of convection artefacts in stimulated-echo diffusion experiments. Double-stimulated-echo experiments, J. Magn. Reson. 125 (1997) 372-375

[18] M.A. Connell, P.J. Bowyer, P.A. Bone, A.L. Davis, A.G. Swanson, M. Nilsson, G.A. Morris, Improving the accuracy of pulsed field gradient NMR diffusion experiments: correction for gradient non-uniformity, J. Magn. Reson. 198 (2009) 121-131

[19] D. Sinnaeve, "Characterisation of the structure and self-assembly of a small cyclic peptide. An analysis using NMR spectroscopy, diffusion and heteronuclear relaxation measurements", Appendix B PhD thesis (2010), Ghent University

[20] C.S. Johnson, Diffusion ordered nuclear magnetic resonance spectroscopy: principles and applications, Prog. Nucl. Magn. Reson. Spectrosc. 34 (1999) 203-256

[21] B. Antalek, Using pulse gradient spin echo NMR for chemical mixture analysis: how to obtain optimum results, Concepts Magn. Reson. 14 (2002) 225-258

[22] J.S. Alper, R.I. Gelb, Standard errors and confidence-intervals in nonlinear-regression – Comparison of Monte-Carlo and parametric statistics, J. Phys. Chem. 94 (1990) 4747-4751

[23] P. Stilbs, G. Arvidson, G. Lindblom, Vesicle membrane-water partition coefficients determined from Fourier-transform pulsed-gradient spin-echo NMR based self-diffusion data – Application to anaesthetic binding in tetracaine-phosphatidylcholine-water systems, Chem. Phys. Lipids 35 (1984) 309-314

[24] V. Suratkar, S. Mahapatra, Solubilization site of organic perfume molecules in sodium dodecyl sulfate micelles: new insights from proton NMR studies, J. Colloid Interface Sci. 225 (2000) 32–38

[25] J.P. Mata, V.K. Aswal, P.A. Hassan, P. Bahadur, A phenol-induced structural transition in aqueous cetyltrimethylammonium bromide solution, J. Colloid Interface Sci. 299 (2006) 910–915

[26] R. Chaghi, L.C. de Menorval, C. Charnay, G. Derrien, J. Zajac, Interactions of phenol with cationic micelles of hexadecyltrimethylammonium bromide studied by titration calorimetry, conductimetry, and ^{1}H NMR in the range of low additive and surfactant concentrations, J. Colloid Interface Sci. 326 (2008) 227–234

[27] K. Xu, H.Q. Ren, G.M. Zeng, L.L. Ding, J.H. Huang, Investigation of interaction between phenol and cetylpyridinium chloride micelle in the absence and in the presence of electrolyte by ^{1}H NMR spectroscopy, Colloid Surf., A 356 (2010) 150-155

[28] D.R. Lide, Handbook of Chemistry and Physics, 73th Edition, CRC Press, 1992, p.8-40.

[29] M.C. Fernandez, P. Fromherz, Lipoid pH-indicators as probes of electrical potential and polarity in micelles, J. Phys. Chem. 81 (1977) 1755-1761

[30] N.O. Mchedlov-Petrossyan, V.N. Kleshchevnikova, Influence of the cetyltrimethylammonium chloride micellar pseudophase on the protolytic equlibria of oxyxanthene dyes at high bulk phase ionic strength, J. Chem. Soc. Faraday Trans. 90 (1994) 629-640

[31] A. Avdeef, K.J. Box, J.E.A. Comer, C. Hibbert, K.Y. Tam, pH-metric logP 10. Determination of liposomal membrane-water partition coefficients of ionizable drugs, Pharm. Res. 15 (1998) 209-215

[32] Y. Wang, C. Combe, M.M. Clark, The effects of pH and calcium on the diffusion coefficient of humic acid, J. Membrane Sci. 183 (2001) 49-60

[33] N. Hedin, R. Sitnikov, I. Furo, U. Henriksson, O. Regev, Shape changes of C_{16}TABr micelles on benzene solubilization, J. Phys. Chem. B 103 (1999) 9631-9639

Figures and tables

Figure 1: ^{1}H-NMR spectra of: a) 10 mM CTAB in D_2O; b) 5 mM phenol in D_2O (pH=6.50); c) 5 mM phenol and 10 mM CTAB in D_2O (pH=6.70)

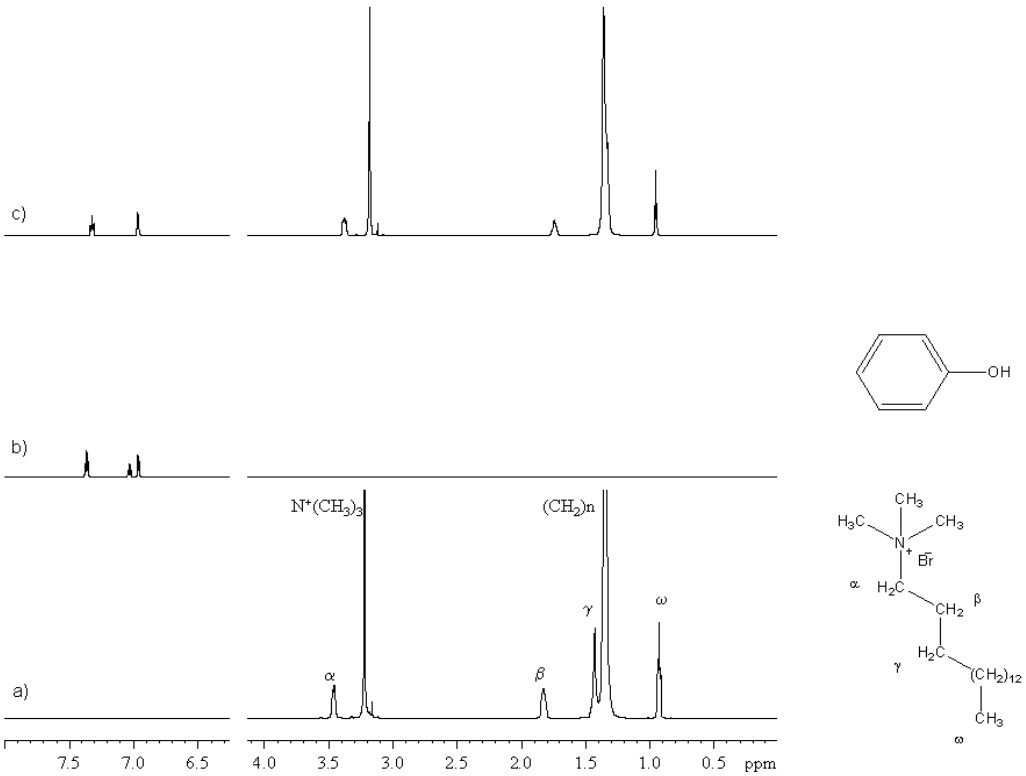

Figure 2: ^{1}H-NMR spectra of 5 mM phenol in D_2O at pH 7.22 (a), 8.30 (b), 9.67 (c), 10.60 (d), and 11.40 (e)

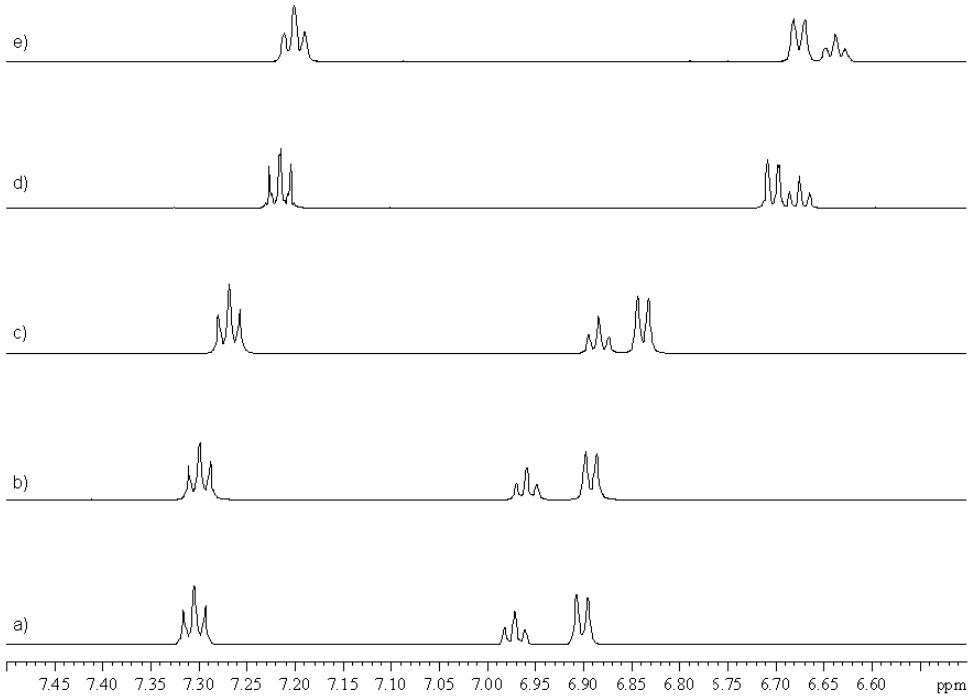

Figure 3: ^{1}H-NMR spectra of 5 mM phenol and 10 mM CTAB in D_2O at pH 8.03 (a), 8.76 (b), 9.30 (c), 9.94 (d), and 12.31 (e).

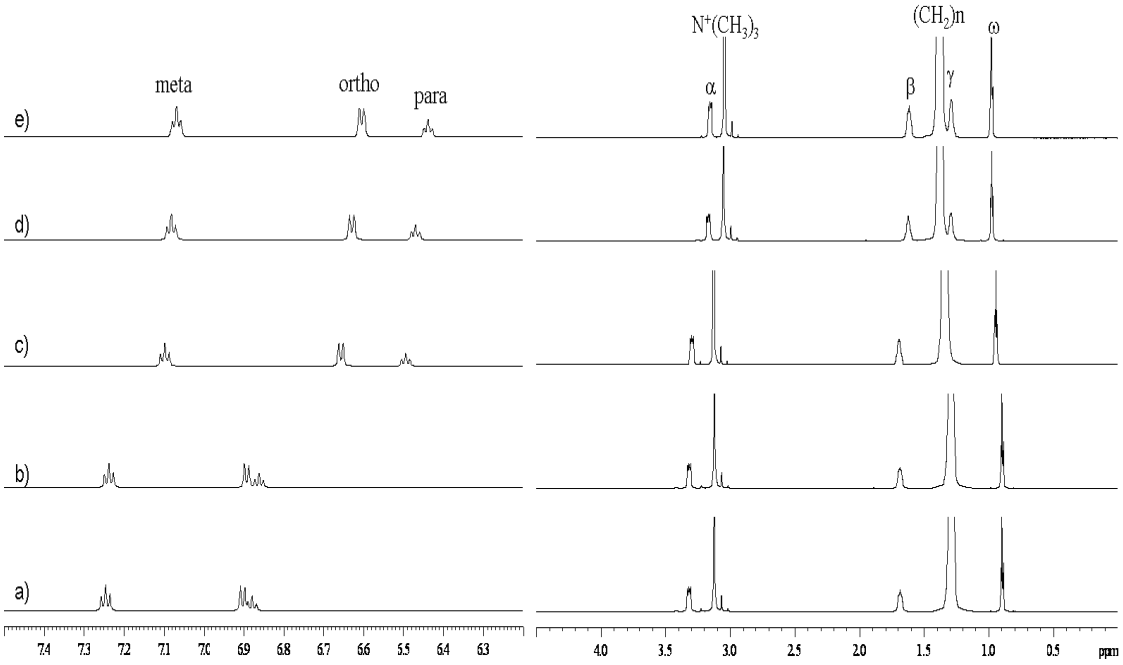

Figure 4: Chemical shift variation of the ortho (▲), meta (♦) and para (■) aromatic protons in a 5 mM phenol solution as function of pH in absence (empty marker) and presence (filled marker) of 10 mM CTAB.

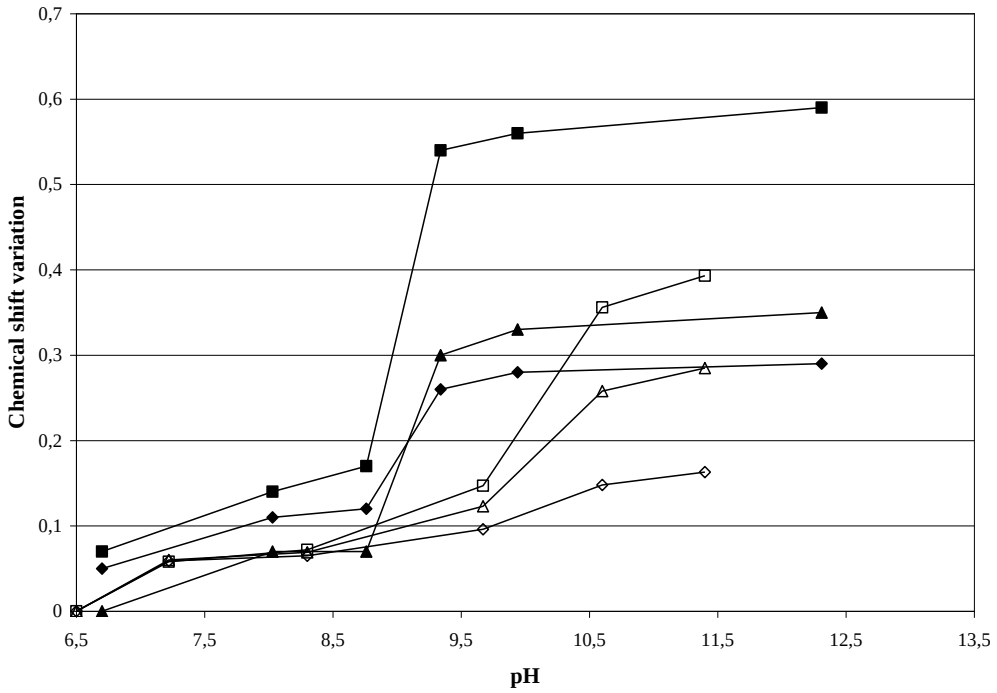

Figure 5: NOESY spectra of 5 mM phenol and 10 mM CTAB in D_2O at pH 6.70 (a), and 9.94 (b).

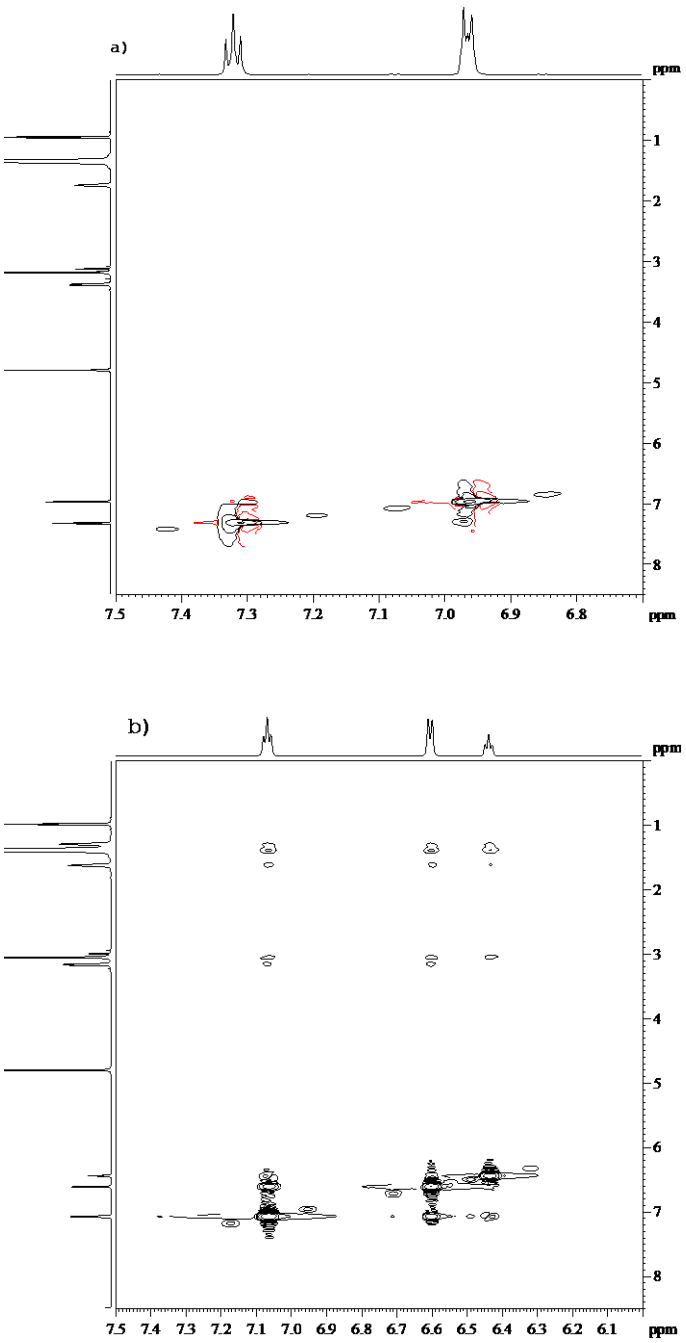

Figure 6: Schematic representation of the solubilization loci of phenol at neutral (a) and high (b) pH

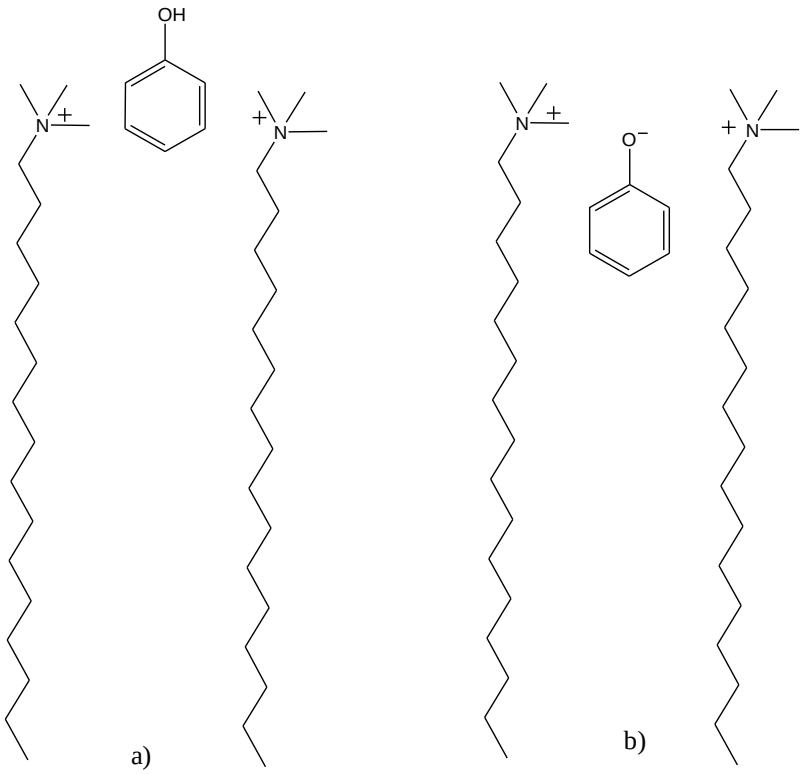

Figure 7: Sorption (with 68% confidence interval) of 5 mM phenol in a 10 mM CTAB micellar solution at 25 °C as a function of pH. The dotted line represents the desorption of phenol upon acidification of the most alkaline sample.

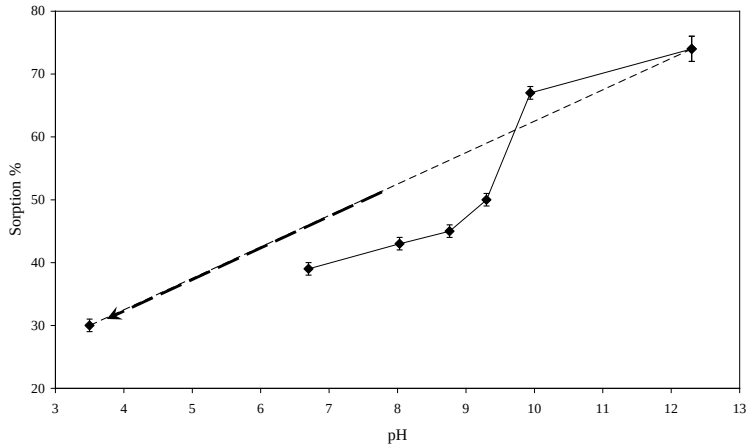

Table 1: Chemical shift difference of protons of 10 mM CTAB in the presence of 5 mM phenol at various pH conditions relative to CTAB without added phenol or NaOH

pH	α-CH_2	$-N^+(CH_3)_3$	β-CH_2	γ-CH_2	Alkyl chain	ω-CH_3
6.70	0.08	0.04	0.09	(›0)*	0.00	-0.01
8.03	0.14	0.10	0.14	(›0)	0.03	0.02
8.76	0.14	0.10	0.14	(›0)	0.03	0.02
9.30	0.16	0.10	0.13	(›0)	-0.01	-0.02
9.94	0.29	0.17	0.20	0.14	-0.04	-0.05
12.31	0.30	0.18	0.21	0.14	-0.05	-0.05

** not possible to estimate because of overlap with alkyl chain signal*

Table 2: Sorption (± standard deviation) of phenol in CTAB micelles in a mixture of 5 mM phenol and 10 mM CTAB at different pH conditions

Diffusion coefficient			**pH**			
[10^{-10} m^2/s]	6.70	8.03	8.76	9.30	9.94	12.31
D_{free}	8.07±0.03	7.88±0.02	7.82±0.03	7.52±0.02	6.53±0.02	6.42±0.04
D_{obs}	5.19±0.01	4.77±0.03	4.60±0.01	4.04±0.02	2.61±0.01	2.18±0.01
D_{mic}	0.63±0.01	0.61±0.01	0.61±0.02	0.61±0.03	0.62±0.04	0.62±0.02
Sorption [%]	39±1	43±1	45±1	50±1	67±1	74±2